REVIEW

National Science Open
2: 20220062, 2023
https://doi.org/10.1360/nso/20220062

Materials Science

Advances of therapeutic microbubbles and nanobubbles

Bin Huang[1,3,#], Li Yang[2,#], Wenbing Yu[1], Yan Li[1], Ling Li[2,*] & Ning Gu[1,3,4,*]

[1]*State Key Laboratory of Bioelectronics, Jiangsu Key Laboratory for Biomaterials and Devices, School of Biological Science and Medical Engineering, Southeast University, Nanjing 210096, China;*
[2]*Zhongda Hospital, Southeast University, Nanjing 210096, China;*
[3]*School of Biomedical Engineering and Informatics, Nanjing Medical University, Nanjing 211166, China;*
[4]*Medical School, Nanjing University, Nanjing 210093, China*

#Contributed equally to this work.
*Corresponding authors (emails: lingli@seu.edu.cn (Ling Li); guning@seu.edu.cn (Ning Gu))

Received 14 October 2022; Revised 15 January 2023; Accepted 29 January 2023; Published online 3 August 2023

Abstract: As versatile nanotools, microbubbles (MBs) and nanobubbles (NBs) have gained increasing attention because of their great potentials for therapeutic applications. The filled gases can greatly influence the physical properties of the MBs and NBs, such as size, zeta potential, and stability. Importantly, the biological activity of the filled gases plays a key role in the therapeutic effect of MBs and NBs. In this review, we will introduce the background, classification, and design strategies of therapeutic MBs and NBs based on bio-active and bio-inactive gases. Furthermore, focus will be placed on the biomedical applications in cancer treatments, including drug delivery, targeting effect and combinations of different therapeutic modalities. Finally, we will discuss the remaining challenges and future perspectives of therapeutic MBs and NBs.

Keywords: microbubbles, nanobubbles, gas, cancer treatment, ultrasound

Introduction

With the rapid development of nanotechnology, various nanoplatforms such as nanomedicine and nano-delivery systems have been explored and developed for the therapy of diseases in clinic over the past few decades [1–6]. Among them, gaseous systems including micro- and nano-sized bubbles with spherical gas-filled and core-shell structures have gained widespread attention because of their distinct advantages, such as flexibility of compositions and structures, favorable and controllable sizes, desirable biocompatibility, high surface area, enhanced permeability and retention, passive targeting and accumulation in lesion region [7–10]. Generally, microbubbles (MBs) have a diameter of more than 1 μm, which is approximately equal to the diameter of a red blood cell. The large size of MBs limits their extravasation from the bloodstream. MBs are traditionally served as ideal ultrasound (US) contrast agents (UCAs) for imaging because of their frequency response to US waves. In medical fields, MBs can also serve as efficient carriers of drugs, gases, genes, etc. Recent studies have shown that the assembled MBs can be transformed into nanoparticles upon US to improve the therapy effect [3]. In contrast, the diameter of nanobubbles (NBs) are decreased to 100 nm–1 μm. Due to the small size, NBs can extravasate from leaky bloodstream into tumor tissues,

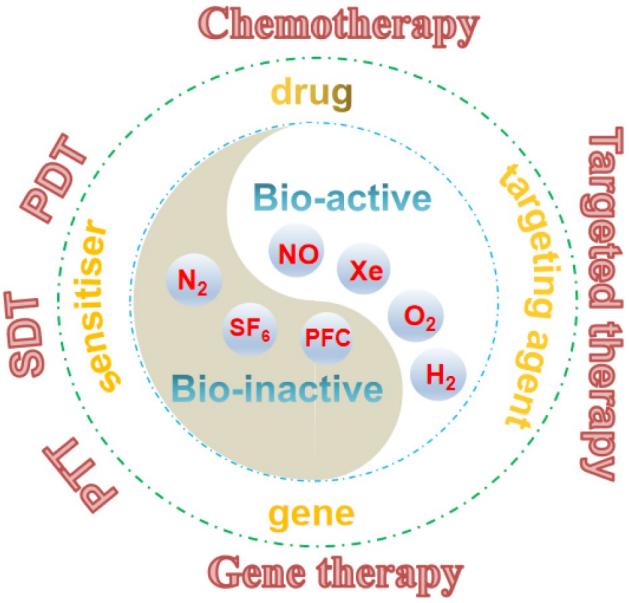

Figure 1 Schematic illustration of therapeutic MBs and NBs for different biomedical applications. Therapeutic MBs and NBs can be classified into two major types: (i) bio-active gases (O_2, NO, Xe, H_2, etc.) based MBs and NBs; (ii) bio-inactive gases (N_2, SF_6, PTC, etc.) based MBs and NBs. Functional substrate such as sensitizer, drug, targeting agent and gene are introduced on the MBs and NBs for enhanced PTT, SDT, PDT, chemotherapy, targeted therapy, and gene therapy.

indicating great potentials for therapeutic applications. Different gases contained in MBs and NBs have an impact on the size, zeta potential, stability, and therapeutic effect. According to the biological activity of the filled gases, MBs and NBs can be classified into two major types (Figure 1): (1) bio-active gases based MBs and NBs; (2) bio-inactive gases based MBs and NBs.

Bio-active gases based MBs and NBs. Some gases such as oxygen (O_2), nitric oxide (NO), xenon (Xe), carbon monoxide, hydrogen and hydrogen sulfide are demonstrated to affect various physiological and pathophysiological processes and involve in some biological activities [3]. For instance, O_2 is well known for respiration to sustain life. Due to the inadequate supply of O_2 to the tissues, hypoxia may occur and lead to various implications. Hypoxia is considered to be the major cause inducing the invasion and metastasis of solid tumor and this phenomenon may restrict the therapeutic effect of chemotherapy, radiotherapy, sonodynamic therapy (SDT), and photodynamic therapy (PDT). O_2 MBs and NBs may provide a facile method to satisfy the urgent need for hypoxia-overcoming treatments [11–20]. As a biological signaling molecule, NO acts as an important regulator in many physiological processes, such as protecting against ischemia-reperfusion injury [21], anti-inflammatory and immunosuppressive effects, reducing platelet aggregation and thrombosis [22], and promoting endothelium regeneration for regulation of the cardiovascular system [23]. However, the therapeutic application of NO depends on its concentration *in vivo*. High concentration (>1 mmol/L) NO in the blood can cause poisoning, while low concentration (10^{-12} to 10^{-9} mol/L) NO in cancer cells may promote cancer cell growth. It is important to achieve controllable delivery and release of NO for clinical translation. NO MBs are born on demand and applied in the treatments of some diseases [24–31]. As a noble gas, Xe is able to traverse the blood-brain barrier due to its small volume and low blood gas partition coefficient [32]. In various hypoxic-ischemic injury cases, Xe is a bioactive gas that has been

demonstrated to have anti-apoptotic effects [33]. Xe also shows neuroprotective properties by inhibiting the *N*-methyl-*D*-aspartate without coexisting neurotoxicity [34]. In addition, Xe has cardioprotective [35] and renoprotective effects [36] *in vivo*. Due to Xe's scarcity and high cost, the primary problem of Xe therapy lies in effective delivery and release of Xe. Liposomes and phospholipid are applied to encapsulate Xe MBs or NBs for the localized delivery of Xe and treatments of some diseases [37–40]. Up to now, due to instability or insecurity, other bioactive gases such as carbon monoxide, hydrogen and hydrogen sulfide based MBs and NBs are seldom reported and applied as therapeutic bubbles.

Bio-inactive gases based MBs and NBs. Different from bio-active gases, some gases such as nitrogen, perfluorocarbon (PFC), and sulfur hexafluoride (SF_6) have no therapeutic functions [3]. These gases based MBs and NBs can assist the therapeutic process and be applied as auxiliary tools for controlled drug release, enhanced diagnostic imaging, etc. [41–57]. In addition, the cavitation of MBs and NBs may induce cell apoptosis. Initially, most of UCAs consist of air or N_2 based MBs [51]. However, these MBs tend to dissolve upon increased pressure. To obtain more stable UCAs, some gases (PFC, SF_6) with reduced solubility are filled in MBs. UCAs containing PFC such as octafluoropropane (C_3F_8) and decafluorobutane (C_4F_{10}) can be detained in the blood stream for enough time after injection because these gases have poor solubility and diffusivity in blood. Nowadays, PFC based MBs and NBs are used to construct efficient delivery system for drugs, photosensitizers, siRNAs, plasmid DNA or their combinations [41–50]. Because of the low solubility and good biological safety, SF_6 is also used to construct MBs and NBs. SF_6 MBs and NBs show good stability and high US echogenicity. Therefore, SF_6 MBs and NBs have been widely studied in both biomedical diagnosis and therapy [51–57].

This review will first introduce the background and classification of therapeutic MBs and NBs. Subsequently, the design strategies of therapeutic MBs and NBs will be summarized. Especially, emphasis will be put on the therapeutic applications of MBs and NBs (Table 1), including drug delivery, targeting effect and combinations of different therapeutic modalities. In the end, the challenges and prospects of therapeutic MBs and NBs will be discussed.

Therapeutic microbubbles and nanobubbles

Bio-active microbubbles and nanobubbles

Oxygen microbubbles and nanobubbles

Figure 2 illustrates the design strategies of O_2 MBs and NBs for biomedical applications. Hypoxia is a vital factor that may restrict the therapeutic effect of solid tumors, and hypoxia-inducible factor 1-α (HIF-1α) is known as an important regulator of O_2 homeostasis and hypoxia adaptation in tumour cells. With the accumulation of HIF-1α, tumour cells may acquire resistance to radiation under hypoxic conditions. Iijima *et al*. [13] demonstrated that the use of O_2 NBs water could overcome the hypoxia-induced resistance via inhibiting the expression of HIF-1α. In this report, stable O_2 NBs with sizes ranging from 2 to 3 nm were fabricated using the ΣPM-5 device. In contrast to the cells (EBC-1 lung tumour and MDA-MB-231 breast tumour cells) grown in medium consisting of distilled water, the tumour cells grown in medium made with O_2 NBs-containing water showed a clear suppression of HIF-1α expression.

Khan and coworkers [14] fabricated lipid-shelled O_2 NBs using a sonication method and assessed the

Table 1 Summary of therapeutic MBs and NBs for different biomedical applications

Materials	Gas types	Advantages	Size	Biomedical applications	Reference
Doxorubicin	O_2 NBs	Chemotherapy	184–207 nm	MDA-MB-231 breast cancer and Hela cervical cancer	[15]
Gas vesicles	O_2 NBs	PDT	300–330 nm	SCC7 carcinoma cancer	[18]
ICG	O_2 NBs	PDT	220 nm	Oral cancer	[20]
Biotin functionalised Rose Bengal	O_2 MBs	SDT	1–2 μm	BxPc-3 pancreatic cancer	[16]
Lipid	NO MBs	Chemotherapy	1.012 ± 0.712 μm	Thrombus and ischemia-reperfusion injury	[21]
Streptavidin	NO MBs	Chemotherapy	0.96 ± 0.07 mm	Immunosuppressive and anti-thrombotic	[22]
Lipid	NO MBs	Chemotherapy	3.85 μm	Proliferation, apoptosis, and migration of the mesenchymal stem cells	[28]
H_2O_2 and L-arginine	NO MBs	Chemotherapy	2.32 ± 0.21 μm	Hyperglycemia theranostics	[30]
Lipid	Xe MBs	Chemotherapy	4.2 ± 0.16 μm	Imaging	[32]
Lipid	Xe NBs	Chemotherapy	225 ± 11 nm	Acute ischemic stroke	[35]
Lipid	Xe MBs	Chemotherapy		Early brain injury	[36]
Lipid	Xe MBs	Chemotherapy		Traumatic brain injury	[40]
Porphyrin/ camptothecin-floxuridine	C_3F_8 MBs and NBs	Chemotherapy and PDT	1 μm (MBs) 30 to 100 nm (NBs)	HT-29 colorectal cancer	[43]
Porphyrin derivatives	C_3F_8 NBs	SDT	144.66 to 199.5 nm	LS 174T colorectal cancer	[42]
Rose bengal	C_3F_8 MBs NBs	SDT	130 nm (NBs)	HT-29 colorectal cancer	[46]
Rose Bengal	C_4F_{10} MBs	SDT	1.2–2.2 μm	LNCaP-Lucprostate cancer	[45]
Folic acid, IR-780 iodide	C_3F_8 NBs	PTT	539–643 nm	U87 xenografts	[48]
Porphyrin, HIF1α-siRNA	C_3F_8 MBs	PDT and gene therapy	1 to 7 μm	Triple negative breast cancer	[45]
Folate	C_3F_8 NBs	Physical targeted therapy	80 to 790 nm	FR-positive cancer	[47]
Doxorubicin	C_3F_8 NBs	Chemotherapy	about 350 nm	Anaplastic thyroid cancer	[41]
Platelet membrane	SF_6 NBs	Chemotherapy	246.57 ± 14.32 nm	Vascular endothelial injury	[56]
Superparamagnetic iron oxide nanoparticles	SF_6 NBs	Chemotherapy	227.40 ± 87.21 nm	Ischemic stroke	[57]
Cas9/sgRNA protein	SF_6 MBs	Gene therapy	1.19 μm	Androgenic alopecia	[58]

expression of HIF-1α under hypoxic conditions *in vitro* experiments on MDA-MB-231 breast tumour cells. In comparison to the control sample, O_2 NBs can supply more O_2 and be used to reverse hypoxia. The results indicate that HIF-1α expression is reduced after the introduction of O_2 NBs. In further work, Khan *et al*. [15] synthesized doxorubicin-loaded O_2 NBs (Dox-NBs-O_2) and evaluated the effectiveness of Dox-NBs-O_2 to MDA-MB-231 breast tumour and HeLa cervical tumour cells. They found that Dox-NBs-O_2 could not only down-regulate HIF-1α and enhance reactive oxygen species (ROS) generation, but also reduce the amount of doxorubicin. Under normal or hypoxic conditions, Dox-NBs-O_2 are verified to be more effective in tumor cells compared with commercially available liposomal Dox and free Dox.

To enhance the SDT effect under hypoxic conditions, McEwan *et al*. [16] investigated an oxygen-carrying MBs conjugate composed of lipid O_2 MBs and a biotin functionalised Rose Bengal sensitizer. Due to the

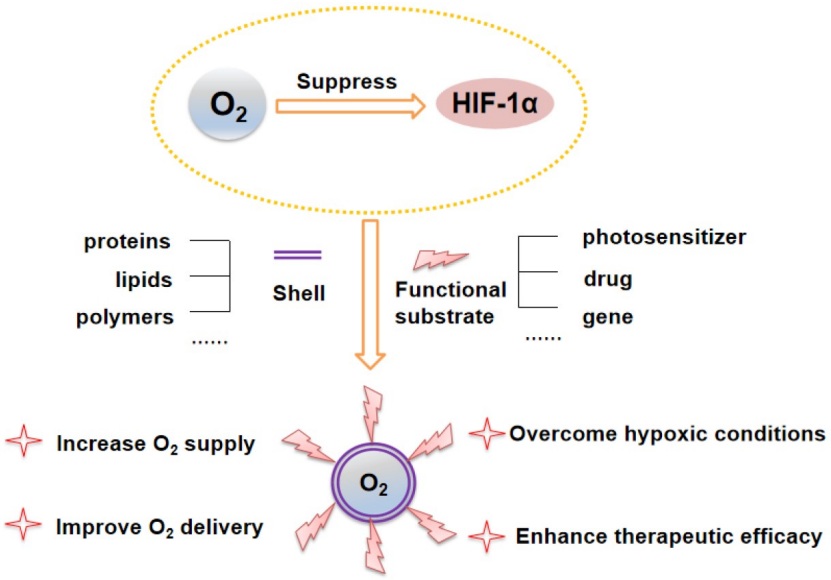

Figure 2 Schematic illustration of the design strategies of O_2 MBs and NBs for biomedical applications. O_2 MBs and NBs can suppress the expression of HIF-1α expression. Stable O_2 MBs and NBs are fabricated by encapsulating O_2 with shells (proteins, lipids or polymers) and functional substrate (photosensitizer, drug or gene). O_2 MBs and NBs can increase O_2 supply, improve O_2 delivery, overcome hypoxic conditions and enhance therapeutic efficacy.

efficient delivery of O_2 to the vicinity of the tumour, the production of ROS is enhanced under US irradiation. For the SDT treatment of BxPc-3 tumour cells, the O_2 MBs conjugate can significantly enhance the therapeutic efficacy due to the combination of O_2 delivery and a US-responsive therapeutic sensitiser on O_2 MBs. Bhandari *et al*. [17] developed O_2 NBs with sizes of 100–200 nm in diameter by encapsulating O_2 inside sodium carboxymethyl cellulose based polymeric shell via a cross-linking step. Through the delivery of O_2, significant hypermethylation can be achieved in promoter DNA region of BRCA1. The release of O_2 inside the hypoxic xenografted MB49 (bladder tumor) and HeLa (cervical tumor) cells may weaken the hypoxia-motivated pathways and suppress tumor growth. In addition, O_2 NBs can also reprogram several hypoxia associated and tumour suppressor genes such as MAT2A and PDK-1. This method is expected to have a significant impact on epigenetic programming and serve as an adjuvant to the treatment of tumours.

Biogenic gas vesicles (GVs) are naturally formed in cynobacteria or archaea and made of protein with stable nanostructure (about 250 nm in diameter) [18]. To improve the stability of O_2 NBs and enhance PDT of hypoxic tumours, Song and coworkers [18] developed O_2-filled GVs as a carrier for effective O_2 delivery. With the addition of O_2-filled GVs, O_2 concentration increased in hypoxic solution and cells, indicating that GVs can carry enough O_2 and have an effect on cell culture. In the presence of O_2-filled GVs, significant enhancement of tumour cell apoptosis and necrosis was observed during PDT.

Indocyanine green (ICG), a clinically near-infrared fluorophore approved by U.S. Food and Drug Administration [19], can serve as a photosensitizer for PDT of tumours. However, a major hurdle of ICG in PDT lies in its poor singlet oxygen ($^1O_2$) production and instability in aqueous solution. To solve these issues, our group [20] developed ICG-NBs-O_2, in which ICG molecules are assembled with O_2 NBs by hydrophilic-hydrophobic interactions. Compared with free ICG, ICG-NBs-O_2 exhibits better stability in solution. Meanwhile, the $^1O_2$ production of ICG-NBs-O_2 is significantly increased to be 1.6%, which is eight times as

high as that of free ICG (0.2%). Furthermore, ICG-NBs-O_2 shows enhanced PDT in the treatment of oral tumours.

Nitric oxide microbubbles

NO can inhibit platelet aggregation by providing an inactivating signal to the protein membrane integrins, thereby controlling arterial thrombosis and cardiovascular disease (Figure 3). However, sometimes the natural supply of NO is insufficient to inhibit blood clotting. Therefore, it is necessary to provide exogenous NO for efficient therapy. Cavalieri *et al*. [24] designed the NO-loaded poly(vinyl alcohol) shelled MBs and investigated the loading capacity and delivery of NO. The results indicate that NO MBs are effective to transport and release NO as anticlotting agent *in vitro*.

NO MBs are also fabricated and used for thrombi treatment [21]. By loading with MBs, the circulation time of NO *in vivo* can be remarkably improved. Moreover, the NO can be released effectively under US radiation. The results show that the thrombus area is significantly reduced and the recanalization rates and blood flow velocities are improved compared with the control group.

High levels of NO have been proved to play a key role in the immune system, mainly through anti-inflammatory and immunosuppressive effects [25]. It is reported that NO can effectively inhibit not only macrophage activation but also the proliferation and recruitment of T and B cells [26,27]. Liao *et al*. [22] developed C4d-targeted NO MBs and used for antibody-mediated rejection studies. Non-invasive diagnosis of antibody-mediated rejection is achieved by quantitative analysis of contrast-enhanced US images after C4d-targeted NO MBs injection. In addition, allograft survival is significantly prolonged and rejection is significantly reduced by inhibiting thrombus formation and reducing inflammatory cell infiltration. Therefore, C4d-targeted NO MBs have shown significantly increased therapeutic efficacy compared with the control group.

Due to the important role of NO in cardiovascular homeostasis, NO MBs have also been studied in the

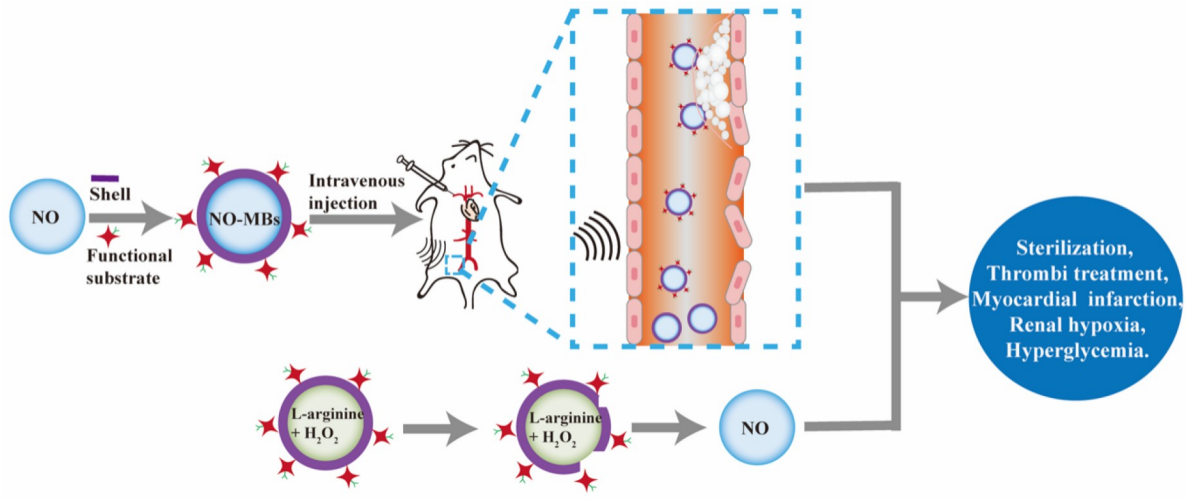

Figure 3 Simplified diagram illustrating functional mechanisms of NO MBs for biomedical applications. NO MBs are stabilized by shells with functional substrates and effective to transport and release NO under US radiation. On the other hand, NO MBs are generated by reacting H_2O_2 with L-arginine *in situ*.

treatment of myocardial infarction [28]. By investigating the effects of US combined with the destruction of NO MBs on the fate of mesenchymal stem cells, it is found that mesenchymal stem cells migrate more efficiently in the group treated with NO MBs under US radiation. Furthermore, the results of the research on the effect of NO MBs on bone marrow mesenchymal stem cells infusion show that NO MBs can be used for cell transplantation and effectively promote the homing of mesenchymal stem cells to the infarcted myocardium upon US irradiation.

NO has been reported to partially mediate signaling in the early stages of glucose-stimulated insulin secretion [29]. However, the delivery and manipulation of NO to biological systems is still relatively difficult because of the reactive chemical nature of NO. Based on glucose and magnetic response, our group [30] developed a theranostic delivery system to generate NO MBs by reacting H_2O_2 with L-arginine *in situ*, which can be used to modulate glucose hemostasis and spatiotemporally control NO release and delivery. On db/db type 2 diabetic mouse model, NO therapy for renal hypoxia is achieved by continuous generation of NO *in situ*. In further work, our group [31] fabricated a nanocarrier by loading L-arginine and γ-Fe_2O_3 magnetic nanoparticles on a natural platelet membrane for targeted delivery of L-arginine and generation of NO *in situ*. Upon the stimulus of magnetic field, the nanocarriers can target ischemic stroke lesions, release L-arginine, and produce NO *in situ*. As a result, generation of NO *in situ* enhances vasodilation and reduces platelet aggregation, which can be used for the therapy of early ischemic stroke.

Xenon microbubbles and nanobubbles

Xe MBs and NBs have great potentials in therapeutic applications (Figure 4). Irani *et al*. [38] fabricated lipid-shelled MBs loaded with Xe by high shear mixing method. The release of gaseous payloads can be triggered using Doppler and pulsed US, and these results suggest the potential application of lipid-shelled MBs in stroke neuroprotection. After intravenous injection of Xe MBs, an US pulse is applied to the carotid artery to release Xe from the MBs into the brain [39]. Based on a high-fidelity pig model, the neuroprotective efficacy of Xe MBs in traumatic brain injury is confirmed.

Because of its ability to diffuse across the blood-brain barrier and safety through expiration, Xe has unique therapeutic advantages in the treatment of ischemic stroke. Recently, our group [35] used phospholipid membrane to encapsulate Xe to construct NBs with sizes of 225 ± 11 nm. Xe NBs are applied to treat acute

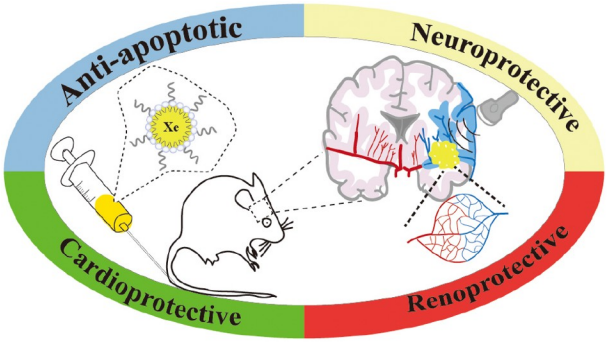

Figure 4 Xe MBs and NBs have anti-apoptotic effects and neuroprotective, cardioprotective and renoprotective properties. More importantly, Xe NBs has unique therapeutic advantages in the treatment of ischemic stroke.

ischemic stroke with neuroprotection and microcirculation restoration. The biodistribution of Xe NBs in mice with ischemic stroke suggests that the enhanced accumulation of Xe NBs in cerebral ischemic lesions may enable contrast-enhanced US imaging with lesion areas and effective delivery of Xe. Compared with the control group, the efficacy of Xe NBs in the treatment of stroke is improved, which provides a new strategy for the therapy of acute ischemic stroke.

Bio-inactive gases based microbubbles and nanobubbles

Perfluorocarbon microbubbles and nanobubbles

PFC MBs and NBs attract increasing attention in the construction of efficient delivery system. To improve the delivery efficacy of doxorubicin and reduce the side effects, doxorubicin-loaded C_3F_8-cored glycol chitosan NBs are designed and fabricated [41]. With the combination of chemotherapy and extracorporeal shock waves under US irradiation, doxorubicin-loaded C_3F_8 NBs exhibit enhanced anti-tumor effects and decreased heart damage. Aimed to obtain efficient theranostic agent for SDT, a series of porphyrin derivatives are loaded on C_3F_8 NBs by manipulating the hydrophilic/lipophilic balance [42]. Under US irradiation, the optimized NBs system exploits the ability to produce ROS and shows a significant reduction in cell viability of LS 174T colorectal cancer.

To conquer multidrug resistance in the chemotherapy of colorectal tumour, Dai's group [43] developed a multimodal therapeutic agent PCF-MBs with high drug loading capacity (w/w: porphyrin 4.5%, floxuridine 14.3% and camptothecin 20.2%) and excellent drug delivery ability. Interestingly, PCF-MBs with sizes of about 1 μm can be converted into nanoparticles with sizes of 30 to 100 nm. Due to the combination of US, chemotherapy and PDT, PCF-MBs can not only significantly reduce the ABCG 2 expression associated with the drug resistance in chemotherapy but also achieve great inhibition of HT-29 colorectal cancer.

Sun *et al*. [44] designed and synthesized multifunctional MBs, siHIF@CpMBs, which contain cationic porphyrin-grafted lipid as a photosensitizer, HIF 1α siRNA as a gene therapy agent for down-regulating the level of HIF 1α and C_3F_8 MBs. siHIF@CpMBs shows a high loading capacity of 24.2% (porphyrin, W/W%) and efficient adsorption of HIF 1α siRNA, indicating its PDT and gene therapy potential. With the destruction of MBs upon US treatment, siHIF@CpMBs is efficiently converted into nanoparticles, leading to the efficient accumulation of porphyrin and siRNA at tumour sites. The results show that knockdown of HIF 1α expression via HIF 1α siRNA can enhance the PDT efficacy and partly inhibit the tumour progression.

To enhance SDT treatment, a Rose Bengal derivative sonosensitizer is covalently attached to the surface of C_4F_{10} MBs. Upon US irradiation, the resulting conjugate shows increased singlet oxygen production and significantly reduces the tumor growth in LNCaP-Luc prostate cancer model [45]. To improve the generation of ROS and delivery efficiency of sonosensitizers in SDT, rose bengal MBs (RB-MBs-C_3F_8) are designed and fabricated by encapsulating C_3F_8 MBs with amphiphilic rose bengal. RB-MBs-C_3F_8 exhibits high drug-loading capability (~6.8%) and good contrast enhancement ability for US imaging, simultaneously. Similar to the PCF-MBs mentioned above, RB-MBs-C_3F_8 can also be transformed to nanoparticles under US irradiation. Compared with the corresponding RB-MBs-C_3F_8 without US irradiation, US-activated RB-MBs-C_3F_8 shows significantly higher drug accumulation and tumour inhibition in HT-29 colorectal cancer model [46].

As a promising strategy, physical non-drug therapy has attracted increasing attention. Based on folic acid

modified *N*-palmitoylc hitosan and C_3F_8 NBs, a novel FNBs-C_3F_8 is designed and fabricated. FNBs-C_3F_8 can effectively target folate receptor-positive tumour cells. Interestingly, FNBs-C_3F_8 can kill folate receptor-positive tumour cells through intracellular explosion upon therapeutic US irradiation [47].

Molecule-targeted UCAs are desirable for accurate diagnosis and targeted therapy of cancer. Multifunctional UCAs based on NBs have attracted increased attention. Shen *et al*. [48] fabricated multifunctional NBs, FA-NBs-IR780, in which a targeting agent folic acid and a near-infrared fluorescence dye IR-780 iodide are assembled on lipid C_3F_8 NBs, respectively. Due to the dual targeting ability, FA-NBs-IR780 can efficiently target tumour cells as expected. More importantly, FA-NBs-IR780 shows striking photothermal responsiveness under 808 nm irradiation and can be used as a photothermal agent for efficient PTT.

Sulfur hexafluoride microbubbles and nanobubbles

To improve the stability of UCAs, people tend to other gases with poor solubility in water. Schneider *et al*. [51] developed BR1, a suspension of SF_6 MBs for efficient UCAs. The MBs in BR1 have a mean diameter of 2.5 μm, a favourable size distribution and high bubbles concentration of 2×10^8 mL^{-1}, resulting in highly echogenic suspensions. Compared with surface NBs, production of stable bulk NBs is still at the initial stage. Recently, our research group [52] developed the repeated compression method for the fabrication of bulk SF_6 NBs. The average particle size of the generated SF_6 NBs is 240 nm and the polydispersity coefficient is 0.25. The SF_6 NBs have a high negative zeta potential with good stability of more than 48 h. Additionally, the formation mechanism of SF_6 NBs was investigated using dark-field microscopy [53]. The dynamic evolution of bulk NBs *in situ* is visualized and traced with dark-field microscopy, and it is directly observed that NBs are formed by the shrinkage of MBs. A comparative study shows that MBs carrying different types of gases (Xe, air, and SF_6) exhibit different shrinkage rates due to their different gas barrier properties. However, the final stable NBs do not differ significantly in sizes and zeta potential. Further, the bubble stabilization mechanism is investigated by the attenuated total reflection Fourier transform infrared spectroscopy. According to the experimental results, it is speculated that the strong hydrogen bonding at the air-water interface may be responsible for promoting the stability of NBs.

SF_6 NBs show excellent potentials in the development of therapeutic nanomaterials (Figure 5). To overcome poor water stability and concentration-dependent aggregation of ICG mentioned above, our group [54] designed and fabricated ICG-NBs-SF_6 by self-assembly of ICG with SF_6 NBs. Compared with free ICG solution, ICG-NBs-SF_6 exhibits increased fluorescence intensity and stability. Very recently, our group [55] prepared SF_6 NBs coated with a high concentration of superparamagnetic iron oxide nanoparticles. US and magnetic resonance imaging experiments show that the assembled magnetic NBs exhibited good contrast between US and magnetic resonance images. In addition, the magnetic NBs are used to label neural stem cells under US excitation. Compared with the ordinary incubation method, the US irradiation method is about twice as efficient as the incubation method.

Platelet membranes have been used in the development of biomimetic diagnostic and therapeutic nanomaterials due to their good biocompatibility and effectiveness. Our group [56] prepared platelet membrane-encapsulated SF_6 NBs with ideal echogenicity by a tunable pressure-induced shear stress method. The results show that high shear stress during the fabrication of platelet membrane-encapsulated SF_6 NBs enables the enrichment of platelet membrane lipid rafts and proteins and their assembly at the air-liquid interface of SF_6

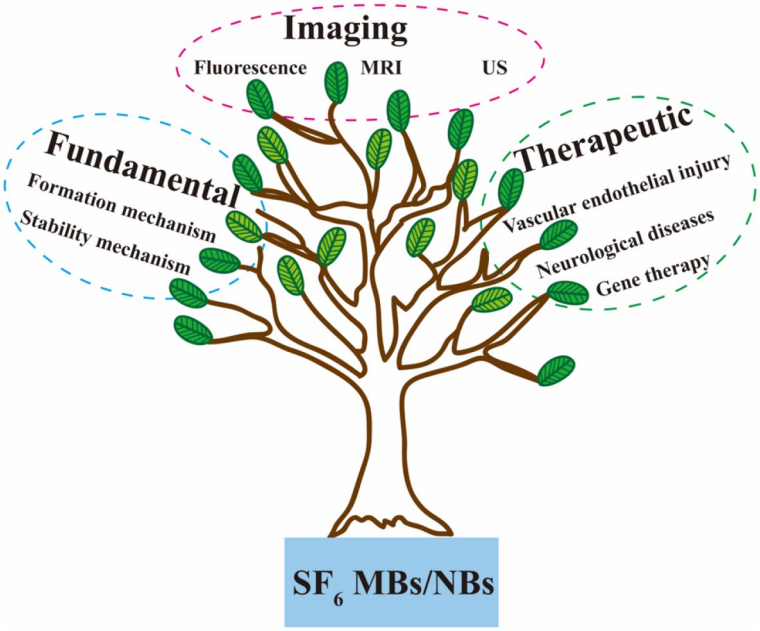

Figure 5 Mindmap of SF_6 MBs and NBs development. The research on SF_6 MBs and NBs mainly involves three aspects: (i) the formation and stability mechanism; (ii) imaging applications include magnetic resonance, fluorescence and ultrasound imaging; (iii) therapeutic applications such as vascular endothelial injury, neurological diseases, and gene therapy.

free bubbles. Due to the conformation shift of platelet integrin αIIbβ3 to a shear stress-induced intermediate-affinity state, platelet membrane-encapsulated SF_6 NBs enhance the ability to adhere to vascular endothelial injury and show great application potential in the specific targeted US diagnosis of vascular endothelial injury.

Neural stem cells (NSCs) have been used in the treatment of various neurological diseases because of their self-renewal ability and multi-directional differentiation potential. However, the tracking of migratory capacity *in vivo* and the control of survival and differentiation efficiency of NSCs are insufficient, limiting the clinical application. To modulate NSCs fate, our group designed and fabricated magnetic NBs-labeled NSCs, in which magnetic NBs assembled from magnetic nanoparticles and SF_6 NBs are internalized by NSCs. In the case of magnetic SF_6 NBs labeled NSCs, intramembrane volume oscillations of magnetic NBs-labeled NSCs may induce increases in intracellular hydrostatic pressure and cytoskeletal force, resulting in Piezo1-Ca^{2+} machinery sensory channel activation. This in turn triggers the BMP2/Smad biochemical signaling pathway, leading to NSCs differentiation into a neuronal phenotype. Signaling through the Piezol-Ca^{2+}-BMP2/Smad pathway can be further accelerated using low-intensity pulsed US. Therefore, it is possible to utilize magnetic NBs-labeled NSCs for efficient NSCs treatment outcomes monitored by magnetic resonance and US imaging [57].

As a non-viral strategy, SF_6 MBs and NBs can be applied to deliver genes with the mediation of US [59]. With the continuous advancement of gene editing technology, combining the CRISPR/Cas9 system with nanocarrier technology can improve the delivery efficiency and biocompatibility of genetic materials. Ryu *et al*. [58] designed SF_6 MBs conjugated nanoliposome system as a Cas9/sgRNA riboprotein complex carrier, which can effectively facilitate local delivery to specific sites under US irradiation. Additionally, the SF_6 MBs conjugated nanoliposome particle can transfer protein complexes into hair follicle cells and exhibit high

efficiency in editing target genes *in vitro* and *in vivo*. Therefore, US-activated SF_6 MBs conjugated nano-liposome particle vectors may help expand the platform for protein-based gene editing.

Conclusions and future perspective

As promising biomedical nanotools, therapeutic MBs and NBs have shown significant potential in clinic for their excellent and unique properties. Therapeutic MBs and NBs are fabricated by sonication, mulsion, mechanical agitation, laser ablation, and other methods [7,36,52]. Compared with therapeutic gas, therapeutic MBs and NBs have measurable sizes and good stability [20]. As mentioned above, some functional MBs and NBs show specific treatments and good efficiency in therapy. However, therapeutic MBs and NBs still have some restrictions on their clinical applications. Some essential issues need to be addressed for the broad applications of therapeutic MBs and NBs.

(1) In comparison to conventional gas therapy, the gases especially bio-active gases involved in therapeutic MBs and NBs remain limited in number. Thus, there is ample room for developing additional types of multifunctional MBs and NBs to expand their therapeutic application. To date, it is still challenging to expand therapeutic MBs and NBs to more bio-active gases through the improvement of materials, methodologies and technologies. Especially, with the breakthrough in molecular mechanism of hydrogen in the body [60], more efforts should put into the development of hydrogen based MBs and NBs for biomedical application.

(2) As efficient nano-delivery systems, the drug loading rate and targeting ability of MBs and NBs should be improved. In general, MBs show better frequency response properties upon US than NBs. In contrast, due to the smaller size for permeating into the vascular wall, NBs possess better passive-targeting ability than MBs. Therefore, more efforts should be made to precisely regulate the sizes of the bubbles for larger drug loading rate, better targeting ability and frequency response properties simultaneously.

(3) Although many therapeutic MBs and NBs have been designed and investigated in clinical treatments, only a limited number of MBs have received FDA approval for clinical application. Therefore, it is urgent to carry out comprehensive clinical evaluation on therapeutic MBs and NBs, which may help accelerate their translation into clinics and fulfill their therapeutic potentials.

Funding

This work was supported by the National Key Research and Development Program of China (2017YFA0104302), the National Natural Science Foundation of China (51832001 and 61821002), the China Postdoctoral Science Foundation Funded Project (2020M681464), and Jiangsu Planned Projects for Postdoctoral Research Funds (2021K601C).

Conflict of interest

The authors declare no conflict of interest.

References

1 Wilhelm S, Tavares AJ, Dai Q, *et al.* Analysis of nanoparticle delivery to tumours. *Nat Rev Mater* 2016; **1**: 16014.

2 Liu D, Yang F, Xiong F, *et al.* The smart drug delivery system and its clinical potential. *Theranostics* 2016; **6**: 1306–1323.

3 Yu L, Hu P, Chen Y. Gas-generating nanoplatforms: Material chemistry, multifunctionality, and gas therapy. *Adv Mater* 2018; **30**: 1801964.

4 Manoharan D, Li WP, Yeh CS. Advances in controlled gas-releasing nanomaterials for therapeutic applications. *Nanoscale Horiz* 2019; **4**: 557–578.

5 He W, Zhang Z, Sha X. Nanoparticles-mediated emerging approaches for effective treatment of ischemic stroke. *Biomaterials* 2021; **277**: 121111.

6 Yang N, Gong F, Cheng L. Recent advances in upconversion nanoparticle-based nanocomposites for gas therapy. *Chem Sci* 2022; **13**: 1883–1898.

7 Wijaya A, Maruf A, Wu W, *et al.* Recent advances in micro- and nano-bubbles for atherosclerosis applications. *Biomater Sci* 2020; **8**: 4920–4939.

8 Duan L, Yang L, Jin J, *et al.* Micro/nano-bubble-assisted ultrasound to enhance the EPR effect and potential theranostic applications. *Theranostics* 2020; **10**: 462–483.

9 Zhang C, Li Y, Ma X, *et al.* Functional micro/nanobubbles for ultrasound medicine and visualizable guidance. *Sci China Chem* 2021; **64**: 899–914.

10 Zahiri M, Taghavi S, Abnous K, *et al.* Theranostic nanobubbles towards smart nanomedicines. *J Control Release* 2021; **339**: 164–194.

11 Cavalli R, Bisazza A, Giustetto P, *et al.* Preparation and characterization of dextran nanobubbles for oxygen delivery. *Int J Pharm* 2009; **381**: 160–165.

12 Swanson EJ, Borden MA. Injectable oxygen delivery based on protein-shelled microbubbles. *Nano LIFE* 2010; **1**: 215–218.

13 Iijima M, Gombodorj N, Tachibana Y, *et al.* Development of single nanometer-sized ultrafine oxygen bubbles to overcome the hypoxia-induced resistance to radiation therapy via the suppression of hypoxia-inducible factor-1α. *Int J Oncol* 2018; **52**: 679–686.

14 Khan MS, Hwang J, Seo Y, *et al.* Engineering oxygen nanobubbles for the effective reversal of hypoxia. *Artif Cells Nanomed Biotechnol* 2018; **46**: 318–327.

15 Khan MS, Hwang J, Lee K, *et al.* Anti-tumor drug-loaded oxygen nanobubbles for the degradation of HIF-1α and the upregulation of reactive oxygen species in tumor cells. *Cancers* 2019; **11**: 1464.

16 McEwan C, Owen J, Stride E, *et al.* Oxygen carrying microbubbles for enhanced sonodynamic therapy of hypoxic tumours. *J Control Release* 2015; **203**: 51–56.

17 Bhandari PN, Cui Y, Elzey BD, *et al.* Oxygen nanobubbles revert hypoxia by methylation programming. *Sci Rep* 2017; **7**: 9268.

18 Song L, Wang G, Hou X, *et al.* Biogenic nanobubbles for effective oxygen delivery and enhanced photodynamic therapy of cancer. *Acta Biomater* 2020; **108**: 313–325.

19 Zhang RR, Schroeder AB, Grudzinski JJ, *et al.* Beyond the margins: Real-time detection of cancer using targeted fluorophores. *Nat Rev Clin Oncol* 2017; **14**: 347–364.

20 Yang L, Huang B, Hu S, *et al.* Indocyanine green assembled free oxygen-nanobubbles towards enhanced near-infrared induced photodynamic therapy. *Nano Res* 2022; **15**: 4285–4293.

21 Liang Z, Chen H, Gong X, *et al.* Ultrasound-induced destruction of nitric oxide-loaded microbubbles in the treatment of thrombus and ischemia-reperfusion injury. *Front Pharmacol* 2022; **12**: 745693.

22 Liao T, Li Q, Zhang Y, *et al.* Precise treatment of acute antibody-mediated cardiac allograft rejection in rats using C4d-targeted microbubbles loaded with nitric oxide. *J Heart Lung Transplant* 2020; **39**: 481–490.

23 Ignarro LJ. Endothelium-derived nitric oxide: Actions and properties. *FASEB j* 1989; **3**: 31–36.

24 Cavalieri F, Finelli I, Tortora M, *et al.* Polymer microbubbles as diagnostic and therapeutic gas delivery device. *Chem Mater* 2008; **20**: 3254–3258.

25 Bogdan C. Nitric oxide and the immune response. *Nat Immunol* 2001; **2**: 907–916.

26 Bogdan C. Nitric oxide synthase in innate and adaptive immunity: An update. *Trends Immunol* 2015; **36**: 161–178.

27 García-Ortiz A, Serrador JM. Nitric oxide signaling in T cell-mediated immunity. *Trends Mol Med* 2018; **24**: 412–427.

28 Tong J, Ding J, Shen X, *et al.* Mesenchymal stem cell transplantation enhancement in myocardial infarction rat model under ultrasound combined with nitric oxide microbubbles. *PLoS ONE* 2013; **8**: e80186.

29 Spinas GA, Laffranchi R, Francoys I, *et al.* The early phase of glucose-stimulated insulin secretion requires nitric oxide. *Diabetologia* 1998; **41**: 292–299.

30 Yang F, Li M, Liu Y, *et al.* Glucose and magnetic-responsive approach toward *in situ* nitric oxide bubbles controlled generation for hyperglycemia theranostics. *J Control Release* 2016; **228**: 87–95.

31 Li M, Li J, Chen J, *et al.* Platelet membrane biomimetic magnetic nanocarriers for targeted delivery and *in situ* generation of nitric oxide in early ischemic stroke. *ACS Nano* 2020; **14**: 2024–2035.

32 Chattaraj R, Hwang M, Zemerov SD, *et al.* Ultrasound responsive noble gas microbubbles for applications in image-guided gas delivery. *Adv Healthc Mater* 2020; **9**: 1901721.

33 Sanders RD, Ma D, Maze M. Anaesthesia induced neuroprotection. *Best Pract Res Clin Anaesth* 2005; **19**: 461–474.

34 Esencan E, Yuksel S, Tosun YB, *et al.* Xenon in medical area: Emphasis on neuroprotection in hypoxia and anesthesia. *Med Gas Res* 2013; **3**: 4.

35 Jin J, Li M, Li J, *et al.* Xenon nanobubbles for the image-guided preemptive treatment of acute ischemic stroke via neuroprotection and microcirculatory restoration. *ACS Appl Mater Interfaces* 2021; **13**: 43880–43891.

36 Miao YF, Peng T, Moody MR, *et al.* Delivery of xenon-containing echogenic liposomes inhibits early brain injury following subarachnoid hemorrhage. *Sci Rep* 2018; **8**: 450.

37 Li Q, Lian C, Zhou R, *et al.* Pretreatment with xenon protected immature rabbit heart from ischaemia/reperfusion injury by opening of the mitoK_{ATP} channel. *Heart Lung Circ* 2013; **22**: 276–283.

38 Irani Y, Pype JL, Martin AR, *et al.* Noble gas (argon and xenon)-saturated cold storage solutions reduce ischemia-reperfusion injury in a rat model of renal transplantation. *Nephron Extra* 2011; **1**: 272–282.

39 Shekhar H, Palaniappan A, Peng T, *et al.* Characterization and imaging of lipid-shelled microbubbles for ultrasound-triggered release of xenon. *Neurotherapeutics* 2019; **16**: 878–890.

40 Hwang M, Chattaraj R, Sridharan A, *et al.* Can ultrasound-guided xenon delivery provide neuroprotection in traumatic brain injury? *Neurotrauma Rep* 2022; **3**: 97–104.

41 Marano F, Frairia R, Rinella L, *et al.* Combining doxorubicin-nanobubbles and shockwaves for anaplastic thyroid cancer treatment: preclinical study in a xenograft mouse model. *Endocrine-Relat Cancer* 2017; **24**: 275–286.

42 Bosca F, Bielecki PA, Exner AA, *et al.* Porphyrin-loaded pluronic nanobubbles: A new US-activated agent for future theranostic applications. *Bioconjugate Chem* 2018; **29**: 234–240.

43 Chen M, Liang X, Gao C, *et al.* Ultrasound triggered conversion of porphyrin/camptothecin-fluoroxyuridine triad microbubbles into nanoparticles overcomes multidrug resistance in colorectal cancer. *ACS Nano* 2018; **12**: 7312–7326.

44 Sun S, Xu Y, Fu P, *et al.* Ultrasound-targeted photodynamic and gene dual therapy for effectively inhibiting triple negative breast cancer by cationic porphyrin lipid microbubbles loaded with HIF1α-siRNA. *Nanoscale* 2018; **10**: 19945–19956.

45 Nomikou N, Fowley C, Byrne NM, *et al.* Microbubble-sonosensitiser conjugates as therapeutics in sonodynamic therapy. *Chem Commun* 2012; **48**: 8332–8334.

46 Hou R, Liang X, Li X, *et al. In situ* conversion of rose bengal microbubbles into nanoparticles for ultrasound imaging guided sonodynamic therapy with enhanced antitumor efficacy. *Biomater Sci* 2020; **8**: 2526–2536.

47 Shen S, Li Y, Xiao Y, *et al.* Folate-conjugated nanobubbles selectively target and kill cancer cells via ultrasound-triggered intracellular explosion. *Biomaterials* 2018; **181**: 293–306.

48 Shen Y, Lv W, Yang H, *et al.* FA-NBs-IR780: Novel multifunctional nanobubbles as molecule-targeted ultrasound contrast agents for accurate diagnosis and photothermal therapy of cancer. *Cancer Lett* 2019; **455**: 14–25.

49 Suzuki R, Takizawa T, Negishi Y, *et al.* Tumor specific ultrasound enhanced gene transfer *in vivo* with novel liposomal bubbles. *J Control Release* 2008; **125**: 137–144.

50 Suzuki R, Namai E, Oda Y, *et al.* Cancer gene therapy by IL-12 gene delivery using liposomal bubbles and tumoral

ultrasound exposure. *J Control Release* 2010; **142**: 245–250.

51 Schneider M, Arditi M, Barrau MB, *et al.* BR1: A new ultrasonographic contrast agent based on sulfur hexafluoride-filled microbubbles. *Investig Radiol* 1995; **30**: 451–457.

52 Jin J, Feng Z, Yang F, *et al.* Bulk nanobubbles fabricated by repeated compression of microbubbles. *Langmuir* 2019; **35**: 4238–4245.

53 Jin J, Wang R, Tang J, *et al.* Dynamic tracking of bulk nanobubbles from microbubbles shrinkage to collapse. *Colloids Surfs A-Physicochem Eng Aspects* 2020; **589**: 124430.

54 Yang L, Huang B, Chen F, *et al.* Indocyanine green assembled nanobubbles with enhanced fluorescence and photostability. *Langmuir* 2020; **36**: 12983–12989.

55 Li J, Feng Z, Gu N, *et al.* Superparamagnetic iron oxide nanoparticles assembled magnetic nanobubbles and their application for neural stem cells labeling. *J Mater Sci Tech* 2021; **63**: 124–132.

56 Li M, Wang L, Tang D, *et al.* Hemodynamic mimic shear stress for platelet membrane nanobubbles preparation and integrin $\alpha_{IIb}\beta_3$ conformation regulation. *Nano Lett* 2022; **22**: 271–279.

57 Li J, Zhang Y, Lou Z, *et al.* Magnetic nanobubble mechanical stress induces the Piezo1-Ca^{2+}-BMP2/Smad pathway to modulate neural stem cell fate and MRI/ultrasound dual imaging surveillance for ischemic stroke. *Small* 2022; **18**: 2201123.

58 Ryu JY, Won EJ, Lee HAR, *et al.* Ultrasound-activated particles as CRISPR/Cas9 delivery system for androgenic alopecia therapy. *Biomaterials* 2020; **232**: 119736.

59 Cavalli R, Bisazza A, Lembo D. Micro- and nanobubbles: A versatile non-viral platform for gene delivery. *Int J Pharm* 2013; **456**: 437–445.

60 Jin Z, Zhao P, Gong W, *et al.* Fe-porphyrin: A redox-related biosensor of hydrogen molecule. *Nano Res* 2023; **16**: 2020–2025.